AC Loss Estimation of HTS Armature Windings for Electric Machines

Min Zhang, M. Chudy, Wei Wang, Yiran Chen, Zhen Huang, Zhaoyang Zhong, Weijia Yuan, J. Kvitkovic, S. V. Pamidi, and T. A. Coombs

***Abstract*—This paper studies 2G high-temperature superconducting (HTS) coils for electric machine armature windings, using finite element method (FEM) and H formulation. A FEM model for 2G HTS racetrack coil is built in COMSOL, and is well validated by comparing calculated ac loss with experimental measurements. The FEM model is used to calculate transport loss in HTS armature windings, using air-cored design. We find that distributed winding used in conventional machine design is an effective way to reduce transport loss of HTS armature winding, in terms of air-cored design. Based on our study, we give suggestions on the design of low loss HTS armature winding.**

***Index Terms*—AC loss, high-temperature superconducting (HTS), machine, YBCO.**

I. Introduction

SUPERCONDUCTING ARMATURE winding was once deemed as unpractical due to the high AC loss and unfeasible cooling capacity [2]. So most of the machine projects focus on superconducting machines with superconducting rotor and conventional copper armature winding [3], [4]. The major drawback of this kind of machine is that the thick cryogenic shell between "cold" rotor and "warm" stator greatly increases the air gap so it reduces the magnetic field in armature windings. Full superconducting machine, enabled by superconducting armature winding, is a much better solution in terms of coupling rotor and stator to produce strong magnetic field [2]. So along with the development of high temperature superconducting (HTS) coils, the idea of superconducting armature winding has flourished again. Economic liquid nitrogen cooling gives hope to HTS armature winding, with projects ongoing all over the world. Our laboratory in University of Cambridge has demonstrated a synchronous motor using 2G HTS racetrack coils as armature winding [5]; Kyoto University has successfully built and tested a fully HTS induction motor with BSCCO as distributed armature winding [6], and is challenging the fabrication of a fully induction motor using M_gB_2 wires [7].

Manuscript received September 28, 2012; accepted January 6, 2013. Date of publication January 11, 2013; date of current version February 27, 2013.

M. Zhang, M. Chudy, W. Wang, Y. Chen, Z. Huang, Z. Zhong, and T. Coombs are with the Engineering Department, Cambridge University, CB3 0FA, U.K. (e-mail: mz279@cam.ac.uk).

J. Kvitkovic and S. V. Pamidi are with Center for Advanced Power Systems, Florida State University, Tallahassee, FL 32310 USA.

W. Yuan is with the Department of Electronics and Electrical Engineering, University of Bath, BA2 7A1, U.K.

Color versions of one or more of the figures in this paper are available online at http://ieeexplore.ieee.org.

Digital Object Identifier 10.1109/TASC.2013.2239341

TABLE I
DOUBLE RACETRACK PARAMETERS

Symbol	Quantity	Value
n	Turns per layer	38
L	Total tape length	39 m
w	Tape width	4 mm
R_1	Inner radius	68 mm
R_2	Outer radius	93 mm

While the projects of HTS winding are prevailing, the need to estimate AC loss of HTS armature winding is urgent and challenging. Numerically, finite element software is extremely popular in calculating AC loss of HTS. Initially, the modeling is focused on single tape: Z. Hong and R. Brambilla *et al.* take the lead in using H formulation for single tape AC loss computation [1], [8], [9]; D. N. Nguyen *et al.* calculate the transport AC loss of YBCO tape with ferromagnetic substrate [10], and magnetization loss when the tape is exposed to a parallel AC magnetic field [11]. Recently, the modeling is more focused on the interaction between tapes such as the modeling of HTS coils. F. Grilli *et al.* use vector potential to simulate stacks of YBCO coated conductors [12]; M. Ainslie *et al.* use H formulation to calculate AC loss for a HTS racetrack coil [16]. We also build an axial symmetrical FEM model for 2G HTS pancakes [13], [14], and find the model consist with experiments.

In this paper, we extend the FEM model in paper [13] to estimate AC loss of 2G HTS racetrack coils used as motor armature windings. The paper is organized as follows: The second section of the paper introduces the FEM model, and validates the FEM model by experimental measurements; the third section studies the transport loss for HTS armature winding; the fourth section discusses the influence of 2G HTS tape performance on their AC loss.

II. The FEM Model and Validation

Double racetrack coil is suitable for making machine armature winding, as shown in Table I the parameters of the racetrack coil we made and used in a synchronous motor [5].

H formulation is applied to the 2D infinite-long model. We have to simplify the racetrack geometry to infinite-long model; we will show below that the infinite-long model simulates the racetrack coil very well. The model contains two variables, defined as $\boldsymbol{H} = [H_x; H_y]$. In 2D geometry, the induced or input current J_z in the superconductor flows in the z direction, so

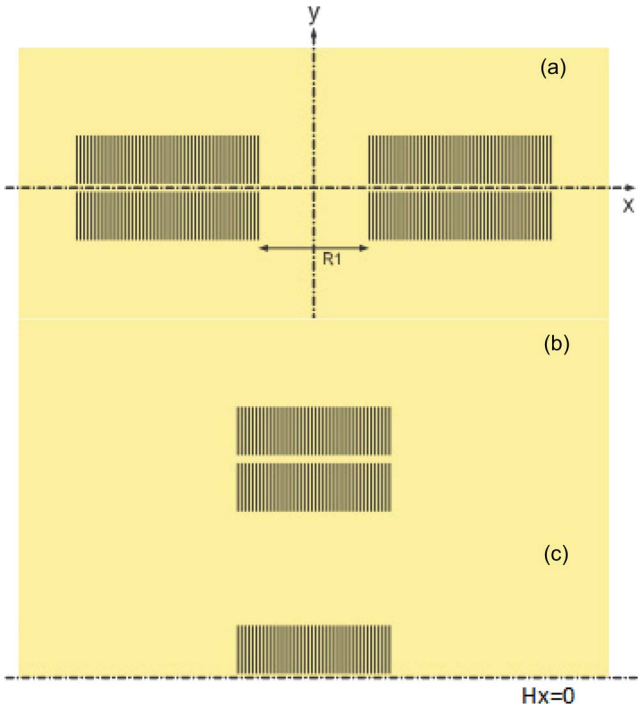

Fig. 1. Cross-section view of the racetrack: (a) whole model and (b) quarter model.

does the electric field $E_z = \rho J_z$, with ρ as the resistivity of the sub-domain.

Ampere's law is written as:

$$J_z = \nabla \times \boldsymbol{H}. \tag{1}$$

Faraday's law is written as:

$$\nabla \times E_z = -\mu_0 \mu_r \, \partial \boldsymbol{H} / \partial t. \tag{2}$$

Combining the equations above, we can solve (3) by finite element software:

$$\mu_0 \mu_r \frac{\partial \boldsymbol{H}}{\partial t} + \nabla \times (\rho \, \nabla \times \boldsymbol{H}) = 0 \tag{3}$$

We have to define resistivity for different materials in the model. For air, we use $\rho = 1000\ \Omega$m. For YBCO, we use the E-J power law: $\rho = E_0 / J_c(B)\ (J_z / J_c(B))^{n-1}$. Other details of the model can be found in our paper [13]–[15].

Fig. 1(a) shows the cross section of the racetrack coil. In the AC loss calculation, we only model the YBCO layer of each turn, which is 1 μm thick in this case. We find from the modeling that $R_1 = 68$ mm of the coil is large enough to decouple the left and right bar of the coil, and ignoring the electromagnetic interaction between them only leads to an error of 2% when the coil is carrying 30 A current. So we manage to simplify the full model from Fig. 1(a) to (b). Without x directional background field, Fig. 1(b) can be further reduced to Fig. 1(c), with only the upper half of the right bar modeled, due to symmetry. Without background field, the boundary conditions are $H_x = 0$ and $H_y = 0$; with background field, the conditions become $H_x = H_{appx}$ and $H_y = H_{appy}$.

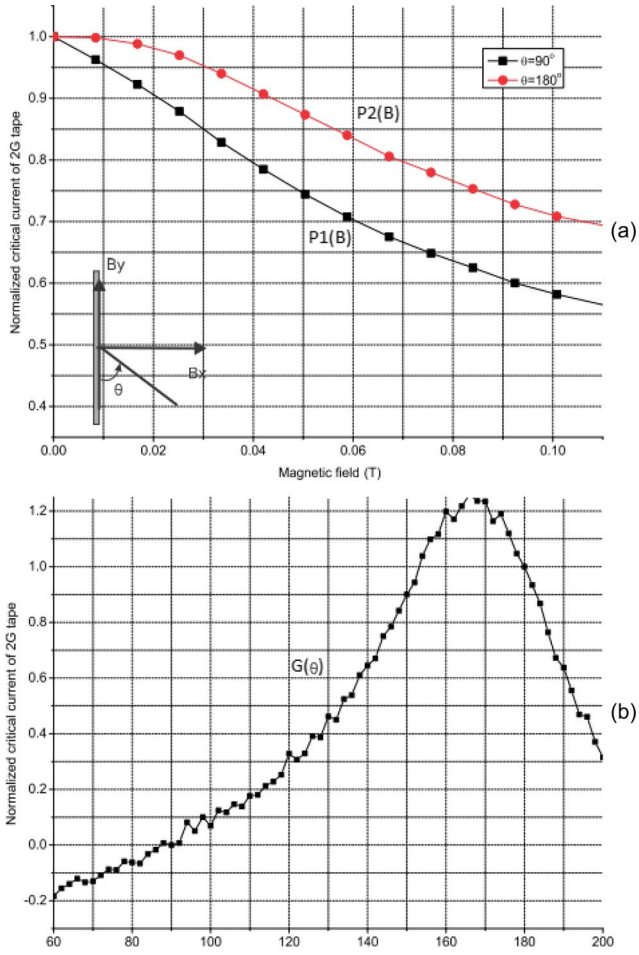

Fig. 2. Normalized experimental data of the tapes' critical currents under (a) perpendicular and parallel field and (b) different field angles of 100 mT.

The influence of magnetic field on the critical current of 2G HTS tape $J_c(B)$ is of paramount importance in the FEM model. We have proposed a well validated method to implement tape anisotropy in COMSOL. Here we briefly introduce the main idea. More details about how to model anisotropic 2G tapes can be found in paper [13].

We measured the magnetic field dependency of 2G tape, with part of the normalized results illustrated in Fig. 2(a). We also measured the angle dependency of critical currents under 100 mT, and normalized the measurement so that $\theta = 180°$ corresponds to the value of 1 and $\theta = 90°$ corresponds to the value of 0. The normalized results are illustrated in Fig. 2(b). The expression used in the model is written in (4), with the explanation of the functions illustrated in Fig. 2.

$$J_c(B) = J_{c0} * \{P1(B) + [P2(B) - P1(B)] * G(\theta)\} \tag{4}$$

when $\theta = 90°$, we have $G(\theta) = 0$, so $J_c(B) = J_{c0} * P1(B)$ gives us the curve with square symbol in Fig. 2(a); when $\theta = 180°$, we have $G(\theta) = 1$, so $J_c(B) = J_{c0} * P2(B)$ gives us the curve with circular symbol in Fig. 2(a). For other θ values, the angle dependency of $J_c(B)$ is modulated by $G(\theta)$, and the magnitude dependency is modulated by $P1(B)$ and $P2(B)$.

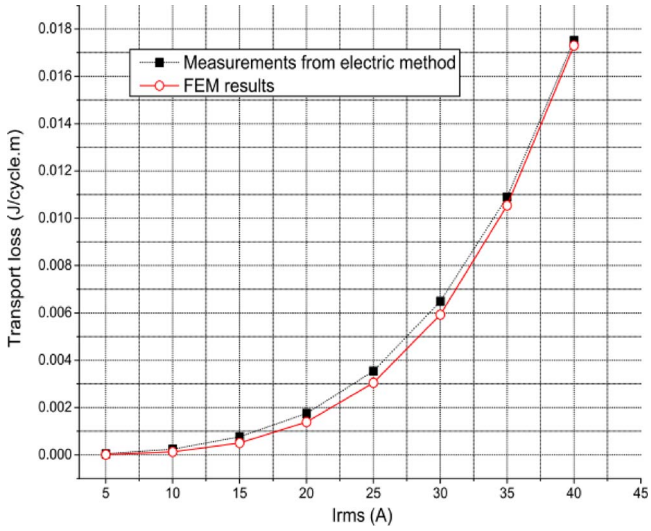

Fig. 3. AC loss of the racetrack coil: comparison of measurements and model results.

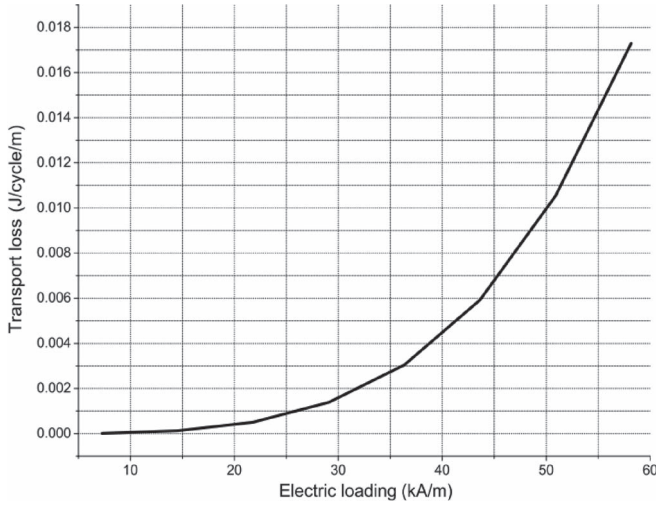

Fig. 4. Electric loading versus transport loss.

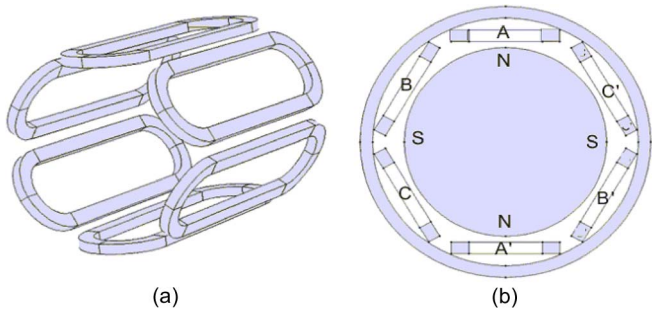

Fig. 5. Armature of the synchronous motor: (a) 3-D geometry of the six racetrack-coils of the armature winding and (b) cross-section view of the motor, with gray area indicating rotor and stator yoke. The mean perimeter of the armature winding is 660 mm, leading to the armature radius $R = 0.105$ m.

The measurements are interpolated into COMSOL directly and used as the functions of (4).

To calculate AC loss $(\mathrm{J} \cdot \mathrm{cycle}^{-1} \cdot \mathrm{m}^{-1})$ from Fig. 3, we integrate $E_z \cdot J_z$ over all the YBCO domains, and then divide it by total turns. We perform loss calculation for 50 Hz AC current, and compare the model results with measurements in Fig. 3. Fig. 3 shows that the model results are consistent with measurements. The experimental results are slightly higher than measurements, which might due to geometry discrepancy, because the end-effect of the racetrack coil cannot be considered in the model. We suggest that the end-effect is the reason for higher measured loss, but further study is required to confirm it. Generally speaking, the FEM model is very accurate in AC loss estimation.

III. Transport Loss Estimation for Armature Winding

Transport loss is closely related to machine electric loading and the arrangement of armature winding. The apparent power output of a machine can be standardly expressed in terms of electric and magnetic loading [2]

$$s = \frac{\pi^2}{\sqrt{2}} k_w B A_s L R^2 \frac{\omega}{p} \quad [\mathrm{VA}] \tag{5}$$

where k_w is the winding factor, B is the average magnetic field density (T), A_s is electric loading (kA/m), L is effective length (m), R is the radius of the machine (m), ω is speed rad/s, and p is the pole pair number. From (5) we learn that the increase of electric loading directly leads to the increase of machine output, and that is exactly the merit of HTS armature winding, to increase machine outputs. Electric loading can vary from 10 kA/m to hundreds of kA/m according to machine size and cooling method. We intend to provide a general idea of the relationship between electric loading and transport loss.

The machine studied has an air-cored armature winding, which suggests that there is no iron in the stator side. 3D and cross-sectional illustrations of such an armature winding is shown in Fig. 5. Assuming that the double racetrack coil mentioned above is used in the armature winding with a pole pitch of 3/4 (which suggests the distance between adjacent coils is 1/4 that of the width of the coil, 68 mm). Based on the design, we are able to plot the loss data in Fig. 3 versus the electric loading, with results shown in Fig. 4. Total transport loss can easily be calculated by multiplying the results in Fig. 4 with the total length of 2G tapes. The tape length of a single coil is 39 m, which gives the total tape length of the armature winding as 234 m. So if the electric loading is designed to be 58 kA/m (corresponding to 40 A AC current) and 50 Hz, the transport loss of the armature winding will be $Q = 0.0173\ \mathrm{J} \cdot \mathrm{cycle}^{-1} \cdot \mathrm{m}^{-1} \cdot 234\ \mathrm{m} \cdot 50\ \mathrm{Hz} = 0.2\ \mathrm{kW}$.

The value of Q is the total transport loss of the machine, giving a general idea of how much loss there is regardless of rotor. However, the magnetic field from the rotor will greatly affect the magnetic field of the armature winding. In real applications of estimating the total loss of the armature winding, the existence of rotor windings cannot be ignored. It can be estimated by applying a background field to the racetrack coil model. The magnitude and direction of magnetic field varies, depending on the rotor design and the air gap length.

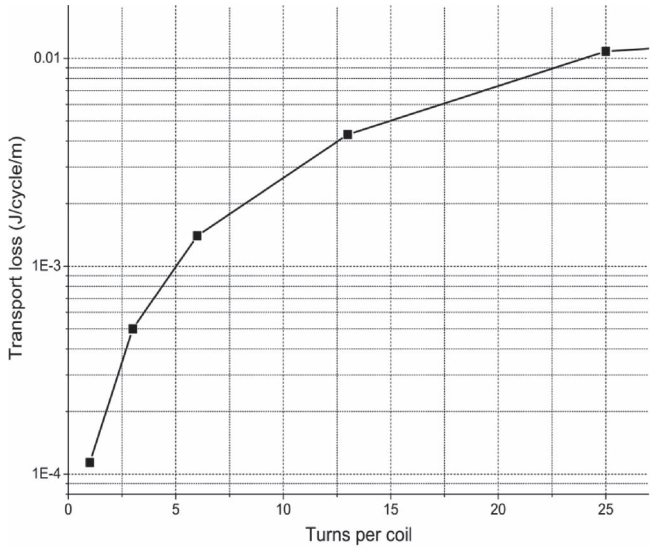

Fig. 6. Transport loss of coils with varied total turns

Specific studies need to be carried out for different machine design.

IV. Armature Loss Reduction

Conventional armature design employs distributed winding to approximate sinusoidal waveforms. So we study the influence of distributed armature winding. We still take electric loading 58 kA/m and 50 Hz as an example. If we divide our 6 racetrack coils into 12, so each coil has 20 turns. Assuming that 12 coils distributed equally along the circumference of the stator, we redesign the motor shown in Fig. 6. The total turn remains unchanged, so the current should be the same to give the same electric loading. We perform transport loss calculation for 20 turns coil carrying $I_{rms} = 40$ A. This time the transport loss reduces to 0.00767 $\mathrm{J \cdot cycle^{-1} \cdot m^{-1}}$, and the total transport loss of the armature winding is 0.09 kW. Comparing to 0.2 kW loss of the concentrated design, the reduction of transport loss reaches 55%. We also test 25, 12, 6, 3, and 1 turn per coil, and the transport losses $(\mathrm{J \cdot cycle^{-1} \cdot m^{-1}})$ are illustrated in Fig. 6. The loss keeps decreasing while we reduce the turns per coil. Given that the total length of the armature winding is fixed to 234 m, we get to the conclusion that fewer turns per coil leads to lower transport loss. In other words, distributed winding helps to reduce AC loss. The reason is that distributed winding reduces the total turns in one coil, as well as the self-field of the coil. The magnetic field affects the critical current density of HTS, as shown in Fig. 2. Lower self-field coil has higher critical current, so for the same applied current, it has lower AC loss.

However, too many distributed coils increase the difficulty and cost of armature manufacture. In this case, 12 coil armature windings would be a good strategy to reduce loss. And also readers should be reminded that we ignore the overlapping of end winding in the case of distributed winding, which might lead to certain amount of loss increase. As long as the coils are long enough and the contribution from end winding can be ignored, our conclusion stands.

V. Conclusion

This paper studied 2G HTS racetrack coil, used as armature winding for electric machine. We built FEM model to simulate 2G HTS coils, with the consideration of 2G tape anisotropy. We well validated the model by comparing transport loss results with experimental measurements by both electric method and calorimetric method. We calculated the transport loss of HTS armature winding in terms of electrical loading of the machine, and we pointed out the distributed winding would be a feasible way to reduce transport loss.

References

[1] Z. Y. Hong, A. M. Campbell, and T. A. Coombs, "Numerical solution of critical state in superconductivity by finite element software," *Supercond. Sci. Technol.*, vol. 19, no. 12, pp. 1246–1252, Dec. 2006.

[2] J. R. Bumby, *Superconducting Rotating Electrical Machines*. New York: Oxford Univ. Press, 1983.

[3] H. W. Neumuller, W. Nick, B. Wacker, M. Frank, G. Nerowski, J. Frauenhofer, W. Rzadki, and R. Hartig, "Advances in and prospects for development of high-temperature superconductor rotating machines at Siemens," *Supercond. Sci. Technol.*, vol. 19, no. 3, pp. S114–S117, Mar. 2006.

[4] R. Ackermann, J. Alexander, A. Gadre, T. Laskaris, K. Sivasubramanium, J. Urbahn, R. Nold, and L. Tomaino, "Testing of a 1.8 MVA high temperature superconducting generator," in *Proc. IEEE Power Eng. Soc. Annu. Meeting*, Toronto, ON, Canada, 2003.

[5] Y. Jiang, R. Pei, W. Xian, Z. Hong, and T. A. Coombs, "The design, magnetisation, control of a superconducting permanent magnetic synchronous motor," *Supercond. Sci. Technol.*, vol. 21, no. 6, pp. 065011-1–065011-6, Jun. 2008.

[6] D. Sekiguchi, T. Nakamura, S. Misawa, H. Kitano, T. Matsuo, N. Amemiya, Y. Ito, M. Yoshikawa, T. Terazawa, K. Osamura, Y. Ohashi, and N. Okumura, "Trial test of fully HTS induction/synchronous machine for next generation electric vehicle," *IEEE Trans. Appl. Supercond.*, vol. 22, no. 3, p. 5 200 904, Jun. 2012.

[7] T. Nakamura, Y. Yamada, H. Nishio, K. Kajikawa, M. Sugano, N. Amemiya, T. Wakuda, M. Takahashi, and M. Okada, "Development and fundamental study on a superconducting induction/synchronous motor incorporated with MgB2 cage windings," *Supercond. Sci. Technol.*, vol. 25, no. 1, pp. 014004-1–014004-7, Jan. 2012.

[8] R. Brambilla, F. Grilli, and L. Martini, "Development of an edge-element model for AC loss computation of high-temperature superconductors," *Supercond. Sci. Technol.*, vol. 20, no. 1, pp. 16–24, Jan. 2007.

[9] Z. Hong, A. Campbell, and T. A. Coombs, "A numerical method to estimate AC loss in superconducting coated conductors by finite element modelling," *Supercond. Sci. Technol.*, vol. 20, no. 4, pp. 331–337, Apr. 2007.

[10] S. P. Ashworth, J. O. Willis, F. Sirois, and F. Grilli, "A new finite-element method simulation model for computing AC loss in roll assisted biaxially textured substrate YBCO tapes," *Supercond. Sci. Technol.*, vol. 23, no. 2, pp. 025001-1–025001-5, Feb. 2010.

[11] D. N. Nguyen, S. P. Ashworth, and J. O. Willis, "Experimental and finite-element method studies of the effects of ferromagnetic substrate on the total ac loss in a rolling-assisted biaxially textured substrat YBCO tape exposed to a parallel ac magnetic field," *J. Appl. Phys.*, vol. 106, no. 9, pp. 093913-1–093913-7, Nov. 2009.

[12] F. Grilli, S. P. Ashworth, and S. Stavrev, "Magnetization AC losses of stacks of YBCO coated conductors," *Phys. C, Supercond.*, vol. 434, no. 2, pp. 185–190, Feb. 2006.

[13] M. Zhang, J.-H. Kim, S. Pamidi, M. Chudy, W. Yuan, and T. A. Coombs, "Study of 2G high temperature superconducting coils: Determination of critical current," *J. Appl. Phys.*, vol. 111, no. 8, pp. 083902-1–083902-8, Apr. 2012.

[14] M. Zhang, J. Kvitkovic, J.-H. Kim, C. H. Kim, S. V. Pamidi, and T. A. Coombs, "Alternating current loss of second-generation high-temperature superconducting coils with magnetic and non-magnetic substrate," *Appl. Phys. Lett.*, vol. 101, no. 10, pp. 102 602-1–102 602-4, Sep. 2012.

[15] M. Zhang, J. Kvitkovic, S. V. Pamidi, and T. A. Coombs, "Experiment and numerical study of YBCO pancake coil with magnetic substrate," *Supercond. Sci. Technol.*, vol. 25, no. 12, pp. 125 020–125 025, Dec. 2012.

[16] M. Ainslie, V. M. Rodriguez-Zermeno, Z. Hong, W. Yuan, T. J. Flack, and T. A. Coombs, "An improved FEM model for computing transport AC loss in coils made of RABiTS YBCO coated conductors for electric machines," *Supercond. Sci. Technol.*, vol. 24, no. 4, p. 045005, Apr. 2011.